

# Learngene Search Across Multiple Datasets for Building Variable-Sized Models

Boyu Shi<sup>1,2</sup>, Junbo Zhou<sup>1,2</sup>, Chang Liu<sup>1,2</sup>, Xu Yang<sup>1,2,\*</sup>,  
Qiufeng Wang<sup>1,2</sup>, Xin Geng<sup>1,2,†</sup>

<sup>1</sup>School of Computer Science and Engineering, Southeast University, Nanjing, China

<sup>2</sup>Key Laboratory of New Generation Artificial Intelligence Technology and Its Interdisciplinary Applications (Southeast University), Ministry of Education, China

\*Co-corresponding author. †Co-corresponding author.

{shiboyu,220242458,liuchang0520,xuyang\_palm,qfwang,xgeng}@seu.edu.cn

## Abstract

Deep learning methods are widely applied in various scenarios with diverse resource constraints, resulting in models of varying sizes, such as the Vision Transformer (ViT) series. Deploying these models typically requires pretraining from scratch followed by finetuning, which is time-consuming and computationally expensive. To address these challenges, the Learngene paradigm has been introduced. This paradigm extracts key components, referred to as learngene, which possess strong learning capabilities, from a well-trained large model, known as the ancestry model (Ans-Net) and uses the learngene to initialize variable-sized models, called descendant models (Des-Nets). Previous methods for extracting learngene focused on a single dataset, which limited the effectiveness of the extraction and resulted in suboptimal performance, particularly in downstream tasks. To overcome this limitation, we propose a novel method for extracting learngene across multiple datasets, called Learngene Search Across Multiple Datasets for Building Variable-Sized Models (LSAMD). LSAMD expands the Ans-Net into a searchable super Ans-Net by introducing dataset-specific blocks and dataset adapters (DADs) in each layer. The dataset-specific blocks learn from the input dataset, while the original blocks in the Ans-Net, called the base blocks remain frozen to retain the initial knowledge. The DAD selects the propagation path between the dataset-specific and base blocks based on the input dataset. During training, LSAMD searches for an optimal architecture path for each dataset from the super Ans-Net. The base blocks most frequently adopted by these paths are then extracted as learngene for initializing variable-sized Des-Nets. Extensive experiments across multiple datasets demonstrate that LSAMD not only achieves performance comparable to the pretrain-finetune method but also significantly reduces both storage and training costs.

## Introduction

Vision Transformers (ViTs) (Dosovitskiy et al. 2020) have made significant advancements in computer vision due to high performance. This capability enables their deployment across a wide range of scenarios, from resource-constrained mobile devices to resource-rich computing centers. The diversity of resource settings results in models of varying sizes. Typically, these models are initialized randomly and

trained from scratch for deploying. However, the training cost associated with this approach increases substantially as the number of deployment scenarios grows.

To address this issue, the Pretrain-Finetune (PF) method has been proposed. This approach involves initially training a source model on a large-scale dataset, such as ImageNet-1K (Deng et al. 2009), and subsequently finetuning the model on target datasets to derive the target model. However, this method requires transferring the entire source model to downstream tasks, which introduces several challenges. For each resource constraint, PF trains a model of a specific size and fine-tunes it for downstream scenarios. As the number of resource constraints increases, the PF method becomes increasingly time-consuming. Besides, PF necessitates storing pretrained models of varying sizes for fine-tuning, leading to significant storage requirements and reduced flexibility for downstream tasks with diverse resource constraints.

Today, a novel learning paradigm called Learngene (Wang et al. 2022, 2023) has been introduced to handle these challenges. The paradigm has two main steps as shown in Figure 1a: (1) Learngene first extracts a small but critical part called learngene from the well-trained large model termed as the ancestry model (Ans-Net). (2) The extracted learngene is then used to initialize variable-sized smaller models, termed descendant models (Des-Nets). Since containing the critical knowledge from the Ans-Net, the learngene has the capability to initialize Des-Nets to perform well on downstream datasets. Besides, the compact scale of learngene allows it to initialize a multitude of diverse medium-sized Des-Nets, thereby exhibiting considerable flexibility in adapting to downstream tasks with varying resource constraints. Since learngene is crucial for the development of Des-Nets, the extraction of appropriate learngene is important. To achieve this, several studies have been conducted to propose methods for extracting learngene from the Ans-Net.

Specifically, Vanilla learngene (Van-LG) (Wang et al. 2022) extracts learngene based on the gradient information of Ans-Net during training across various tasks derived from a single dataset, such as Cifar100 (Krizhevsky 2009) or ImageNet100 (Deng et al. 2009). Additionally, Auto-Learngene (AL) (Wang et al. 2023) trains a meta-network to calculate the similarity between the output of each layer of the Ans-Net and the auxiliary models on Cifar100 (Krizhevsky 2009) or ImageNet100 (Deng et al. 2009), and selects the most

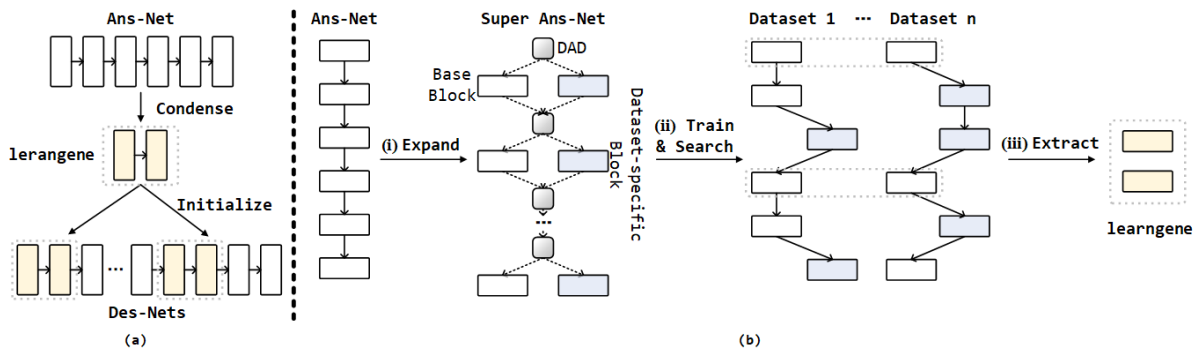


Figure 1: (a) The framework of Learngene. The Ans-Net refers to the ancestry model, and the Des-Nets are descendant models. (b) The overall steps of extracting learnergene in LSAMD. (i) We expand the Ans-Net into the super Ans-Net by adding extra dataset-specific blocks and dataset adapter (DAD). (ii) The super Ans-Net is trained on multiple datasets and we search a specific path for each dataset. (iii) Among these paths, the mostly used blocks from the Ans-Net are extracted as learnergene.

similar layer in the Ans-Net as learnergene. PEG (Wang et al. 2024) employs a probabilistic mixture approach to sample a subset of Multi-Head Self-Attention and Feed-Forward layers from Ans-Net as learnergene, utilizing ImageNet-1K (Deng et al. 2009). LearnGenePool (Shi et al. 2024), TLEG (Xia et al. 2024a), SWS (Xia et al. 2024c) and LeTs (Xia et al. 2024b) distill the Ans-Net into one or more smaller auxiliary models using a single dataset, ImageNet-1K (Deng et al. 2009), to extract learnergene. However, these studies has the following limitation. They extract learnergene from a **single dataset**. One dataset typically follows a specific data distribution, which limits the definition of critical part with general knowledge from the Ans-Net and results in reduced performance of Des-Nets initialized by learnergene.

Motivated by this problem, we propose a new method called **Learngene Search Across Multiple Datasets (LSAMD)** to extract learnergene from the Ans-Net on multiple datasets. The proposed LSAMD involves the following stages. As shown in Figure 1b (i), we first **expand** the architecture of the Ans-Net into a super Ans-Net. In each layer of the super Ans-Net, it additionally incorporates a dataset-specific block and a Dataset Adapter (DAD). The dataset-specific block is initialized with the same parameters as the original block of the Ans-Net, termed as the base block. The DAD determines the forward propagation path between base and dataset-specific blocks when training the super Ans-Net. Then, as shown in Figure 1b (ii), we train the super Ans-Net on multiple datasets. During this process, dataset-specific blocks are updated while base blocks remain fixed, which allows each layer to either learn dataset-specific knowledge or utilize the existing capabilities of Ans-Net. After training, DAD **searches** a specific propagation path for each dataset from the super Ans-Net. We then conduct a layer-wise statistical analysis of the usage frequency of base blocks across all searched paths. Based on this, each base block in the Ans-Net is categorized into one of two scenarios: heavily used, or lightly used. The heavily used base blocks are identified as the critical modules shared across datasets and **extracted** as learnergene, as illustrated in Figure 1b (iii). Finally, we utilize

the extracted learnergene to initialize variable-sized models for downstream tasks with various resource constraints.

Our main contributions are as follows: (1) We extend learnergene extraction from a single dataset to multiple datasets. To the best of our knowledge, this is the first work in the Learngene paradigm to consider a multi-dataset scenario. (2) We introduce a method called LSAMD for searching learnergene from the expanded Ans-Net across multiple datasets. (3) Extensive experiments demonstrate that LSAMD can flexibly build variable-sized models, achieve performance comparable to the pretrain-finetune approach while using less storage and reduce training costs on the downstream tasks.

## Related Work

### Mixture of Experts (MoE)

The Mixture of Experts (MoE) technique, initially proposed by Jacobs et al. (Jacobs et al. 1991), enhances efficiency by combining multiple sub-models and performing conditional computation. Recent research in natural language processing (Shazeer et al. 2017; Chen et al. 2024), vision (Riquelme et al. 2021; Wu et al. 2022; Liu et al. 2024), and multi-modal (Lin et al. 2024; Akbari et al. 2023) applications has adopted sparse MoE techniques to reduce computational costs and train large-scale models. Unlike traditional expert models, modern MoE methods like the Memory Mixture of Experts (MMoE) (Ye and Xu 2023) dynamically assembles task-specific features during multi-task training, significantly enhancing multi-task prediction capabilities. Switch Transformer (Fedus, Zoph, and Shazeer 2022) leveraged distributed training mechanisms and expert sharing techniques. In this paper, we are inspired the MoE method and propose a novel learnergene extraction method to decide the propagation path between dataset-related and base blocks.

### Learngene

The Learngene involves two key stages: condensing learnergene from the Ans-Net, constructing the Des-Net using these learnergene and fine-tuning the Des-Net on downstream

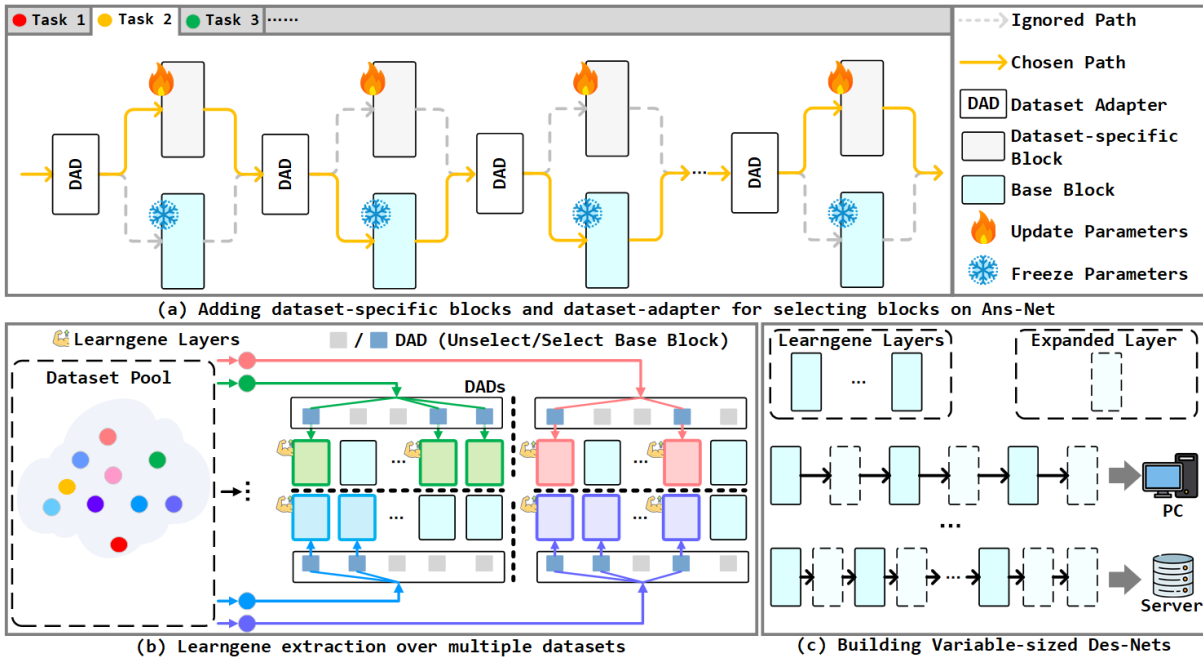


Figure 2: The framework of LSAMD. (a) Each layer of the super Ans-Net consists of a dataset-specific block, a base block and a dataset adapter (DAD). (b) Training the Ans-Net on multiple datasets and extract the base blocks which are used by mostly datasets (marked as muscle) as learnngene layers based on the chosen of DADs. (c) Variable-sized Des-Nets are built by expanding learnngene layers for various resource constraints.

datasets with minimal steps. The vanilla Learngene (Van-LG) (Wang et al. 2022) identifies high-level layers as learnngene based on the gradient information from Ans-Net during training on multiple tasks. These learnngene is combined with a variable number of randomly initialized low-level layers to create Des-Nets of different sizes. Auto-Learngene (Wang et al. 2023) trains pseudo Des-Nets and employs a meta-network to automatically select Ans-Net layers most similar to the pseudo Des-Nets as learnngene. Learngene Pool (Shi et al. 2024) distills the Ans-Net into multiple smaller models, using their layers as learnngene instances to build a pool from which Des-Nets are constructed. TLEG (Xia et al. 2024a) distills Ans-Net into layers that are expanded linearly to create Des-Nets of varying depths. PEG (Wang et al. 2024) samples Multi-Head Self-Attention and Feed-Forward layers from Ans-Net as learnngene using a probabilistic approach, expanding them through non-linear mapping to form Des-Nets. SWS (Xia et al. 2024c) distills Ans-Net into a single model with multiple stages, sharing layer weights, where each stage’s layers serve as learnngene to guide Des-Net expansion. However, these methods extract learnngene from a single dataset, limiting their effectiveness and ultimately impacting the performance of the expanded Des-Nets.

## Methodology

To overcome these limitations, we introduce a new approach called LSAMD, detailed in Figure 2. In this section, we outline LSAMD by focusing on two main aspects: search-

ing learnngene from the Ans-Net using multiple datasets, and building variable-sized Des-Nets based on the learnngene.

### Learngene Search Across Multiple Datasets

**Adding dataset-specific blocks to the Ans-Net.** We first employ DeiT-Base (Touvron et al. 2020) as the Ans-Net, as its larger number of parameters enables it to acquire extensive knowledge from pre-trained datasets. Subsequently, we use  $M$  datasets,  $T_1, T_2, \dots, T_M$ , with varying data distributions to extract learnngene. To enable the Ans-Net to learn dataset-specific knowledge while retaining its original capabilities, we introduce an additional component called the dataset-specific block ( $h_i^D$ ), which operates in parallel with the original block called the base block ( $h_i^B$ ) in each layer of the Ans-Net, as illustrated in Figure 2a. Since randomly initialized dataset-specific blocks have limited learning capacity compared to the well-trained base blocks, this setup could disadvantage the dataset-specific blocks during training. To address this, we share the same architecture and initial parameters between the dataset-specific blocks and base blocks in each layer of the Ans-Net. During training, for each dataset, we update the parameters of the dataset-specific blocks, while keeping the base blocks frozen. This approach ensures that the base blocks remain unaffected by dataset-specific knowledge. Additionally, to prevent interference between the two blocks, we enforce a mechanism that selects only one block per layer for propagation based on the input data.

**Adding dataset adapter to the Ans-Net.** To select be-

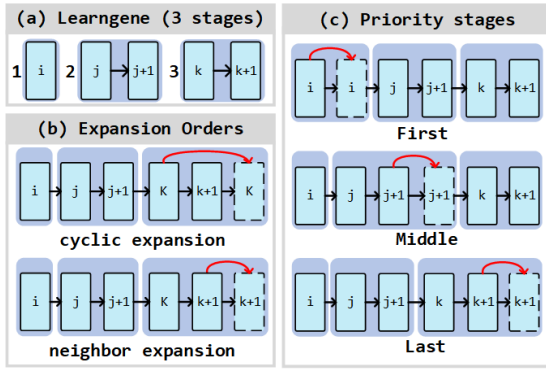


Figure 3: (a) Splitting the learnGene layers into 3 stages. (b) Two kinds of expansion orders. (c) Three priority expansion stages.  $j/j+1$  and  $k/k+1$  are adjacent learnGene layers. We take 5-layer learnGene and 6-layer Des-Net as an example

tween the two blocks, inspired by the Mod-Squad approach (Chen et al. 2022), we introduce a router-like module called the Dataset Adapter (DAD). The DAD determines the propagation path by selecting between the dataset-specific and base blocks, as shown in Figure 2a. For the  $i^{th}$  layer, given input data  $x_t \in \mathbb{R}^{N \times D}$  from the  $t^{th}$  dataset, DAD generates probabilities for each block based on the input:  $P(h_i^D|x_t)$  and  $P(h_i^B|x_t)$  using the following process:

$$P(h_i^D|x_t), P(h_i^B|x_t) = \text{softmax}(x_t W_1 + \text{softplus}(x_t W_2)), \quad (1)$$

where  $W_1 \in \mathbb{R}^{D \times 2}$  represents the weight matrices in DAD, and  $W_2 \in \mathbb{R}^{D \times 2}$  are noisy weight matrices that enhance DAD’s robustness (Shazeer et al. 2017). The  $\text{softplus}(\cdot)$  function smooths the ReLU operation:

$$\text{softplus}(x) = \log(1 + e^x). \quad (2)$$

In each layer, if more than half of the samples in a batch have a higher probability for a specific block, that block becomes the selected propagation path. For instance, if DAD assigns a higher probability to the base block for more than 50 out of 100 images in a batch, the base block is selected, and the dataset-specific block is ignored. Alternatively, as Mod-Squad proposes, each sample can independently forward to corresponding block based on the probability, and the outputs from both blocks are concatenated. However, this approach has been found to yield lower performance compared to the method employed here, as discussed in Section . After adding the data-specific block and the DAD, the Ans-Net becomes a searchable architecture called the super Ans-Net.

**Dataset-Adapter for searching paths over multiple datasets.** Then, we train the super Ans-Net on multiple datasets, as illustrated in Figure 2b. During training, DAD searches between dataset-specific and base blocks in each layer, and DAD returns the corresponding search path based on the input dataset at the end of training. In these paths, we calculate the usage of the searched base blocks by compar-

ing  $P(h_i^D|x_t)$  and  $P(h_i^B|x_t)$ :

$$G_i = \sum_{t=1}^M g_i(t), \quad (3)$$

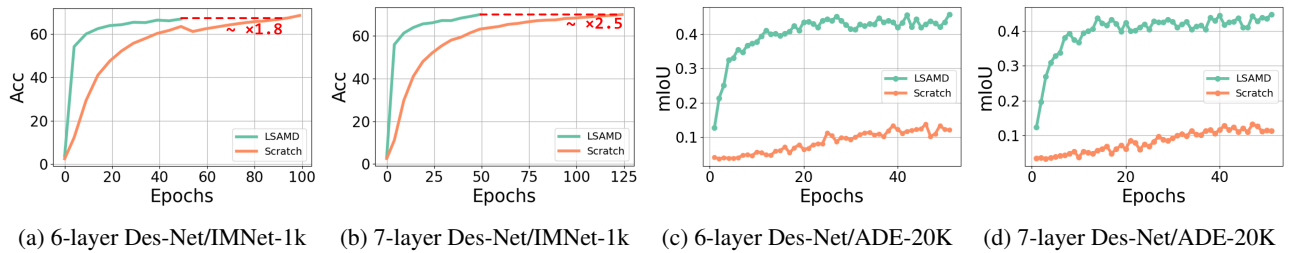
$$\text{s.t. } g_i(t) = \begin{cases} 1, & \text{if } P(h_i^B|x_t) \geq P(h_i^D|x_t) \\ 0, & \text{otherwise} \end{cases}$$

Here,  $g_i(t) \in \{0, 1\}$  indicates whether the  $i^{th}$  base block is used on the  $t^{th}$  dataset, and  $G_i$  represents the total usage of the  $i^{th}$  base block across all datasets. We then divide the searched base blocks into two scenarios: heavily used and lightly used, depending on whether they are used by more than  $\tau \in \mathbb{Z} \cap [1, M]$  datasets. In this paper, we set  $\tau$  to  $M/2$  for ensuring that base blocks used by more than half of the datasets, which helps identify blocks from the Ans-Net that are most consistently shared across diverse datasets. Based on the generality of these heavily used blocks, we extract them as “learnGene” layers. For example, as shown in Figure 2b, the first and third base blocks are selected as learnGene layers because they are utilized by more than half of the datasets. In this study, we take 12 datasets (10 classification datasets and 2 segmentation datasets) for diversity. Here, we set  $\tau = 6$ , which corresponds to half the total number of 10 datasets, and the extracted learnGene layers are indexed at 1, 4, 5, 7, and 8.

While our method, LSAMD, is inspired by the routing mechanisms in Mixture-of-Experts (MoE), its fundamental goal and implementation are distinct. MoE aims to accelerate inference by sparsely activating task-specific experts. In contrast, LSAMD follows the LearnGene paradigm to extract a core set of foundational components from a large Ans-Net for efficiently initializing smaller, resource-adaptive Des-Nets. This distinction in purpose leads to three key differences. First, in terms of granularity, LSAMD performs coarse-grained routing between entire blocks to identify a set of reusable layers, whereas MoE conducts fine-grained routing among MLPs within a block. Second, regarding scope, LSAMD seeks foundational blocks reused across datasets, while MoE selects experts per-dataset for specialized execution. Finally, in architectural impact, LSAMD reduces the model’s core depth to enable flexible scaling, while MoE retains the full model depth, only reducing the activation width during inference.

### Building Variable-Sized Des-Nets

After extracting learnGene layers, we construct variable-sized Des-Nets by replicating and adding these layers, as illustrated in Figure 2c. Since learnGene layers retain both critical knowledge and positional information, we preserve their original order from the Ans-Net and organize them into stages, where adjacent learnGene layers form a single stage, as shown in Figure 3a. Within stages containing multiple blocks, there are two expansion options: cyclic expansion and neighbor expansion. Cyclic expansion replicates learnGene layers in their original sequence within the stage, as depicted in Figure 3b top. Neighbor expansion duplicates the last learnGene layer of the stage, as shown in Figure 3b bottom. Given that neighbor expansion better preserves the



(a) 6-layer Des-Net/IMNet-1k (b) 7-layer Des-Net/IMNet-1k (c) 6-layer Des-Net/ADE-20K (d) 7-layer Des-Net/ADE-20K

Figure 4: Comparison of Scratch and LSAMD on Des-Nets with 6 and 7 layers on IMNet-1K and ADE-20K datasets.

Layer	Method	Cifar100	Cifar10	Pets
6	SWS	80.39	94.87	75.94
	TLEG	77.01	94.27	64.44
	SLAMD	<b>82.77</b>	<b>96.67</b>	<b>79.86</b>
7	SWS	82.19	95.99	81.09
	TLEG	80.03	95.81	74.60
	SLAMD	<b>84.38</b>	<b>97.42</b>	<b>81.34</b>
8	SWS	83.61	96.54	80.25
	TLEG	81.40	96.43	76.35
	SLAMD	<b>83.78</b>	<b>96.74</b>	<b>80.90</b>

Table 1: Comparisons between LSAMD and SWS, TLEG on 4 downstream datasets of Des-Nets with various layer.

original order and learning process of the Ans-Net, we adopt this method for expansion.

Furthermore, it is also crucial to prioritize which stages of the learnene layers to expand. For Des-Nets with the same number of layers, we consider three expansion priorities: the first, middle, or last stage, as illustrated in Figure 3c. Our investigation, detailed in Section , shows that expanding in the last-middle-first priority order yields the best results for the Des-Nets, and we take this priority in our methods.

## Experiments

### Experimental Setup

We train the super Ans-Net by the following 12 datasets: Cifar100 (Krizhevsky 2009), Cifar10 (Krizhevsky 2009), Tiny-ImageNet (Ti-IMNet) (Le and Yang 2015), INAT2019 (Horn et al. 2017), Food101 (Bossard, Guillaumin, and Gool 2014), Cars196 (Krause et al. 2013), Flowers102 (Nilsback and Zisserman 2008), Pets (Parkhi et al. 2012), DTD (Cimpoi et al. 2013), Caltech101 (Fei-Fei, Fergus, and Perona 2004), VOC12 (Everingham et al. 2015), and ADE-20K (Zhou et al. 2019, 2017). The overview information of these ten datasets and the training details are shown in the supplementary material.

### Main Results and Analysis

**LSAMD vs. Scratch.** We compare the performance of LSAMD and training from scratch (Scratch) on 6-layer and 7-layer Des-Nets on the ImageNet-1K (IMNet) (Deng et al. 2009) dataset, as shown in Figure 4. It can be observed that



(a) Cifar10

(b) Cifar100

Figure 5: Performance comparison of Scratch, Pretrain-Finetune (PF) and LSAMD on 10-layer Des-Nets across 4 downstream image classification dataset.

LSAMD achieves superior performance on both 6-layer and 7-layer Des-Nets and both tasks. Specifically, when training a 6-layer Des-Net, LSAMD reduces training costs by approximately **1.8x** while reaching comparable performance, as illustrated in Figure 4a. Similarly, for the 7-layer Des-Net, LSAMD achieves a cost reduction of around **2.5x**, as depicted in Figure 4b. These results highlight the advantage of LSAMD over the Scratch method on the ImageNet-1K dataset. Moreover, as the number of layers in Des-Net increases, the training cost savings become more significant. This trend demonstrates the scalability of LSAMD and its suitability for scenarios with fewer resource constraints. Moreover, we also compare LSAMD and training from scratch on the semantic segmentation task. As shown in Figure 4c and Figure 4d, both Des-Nets initialized by LSAMD maintain excellent results compared to the training from scratch.

Furthermore, We train the 10-layer Des-Net from scratch (Scratch) for 300 epochs and compare it with the same Des-Net initialized using LSAMD, which is trained for only 50 epochs on Cifar10, Cifar100, Pets and DTD. As illus-

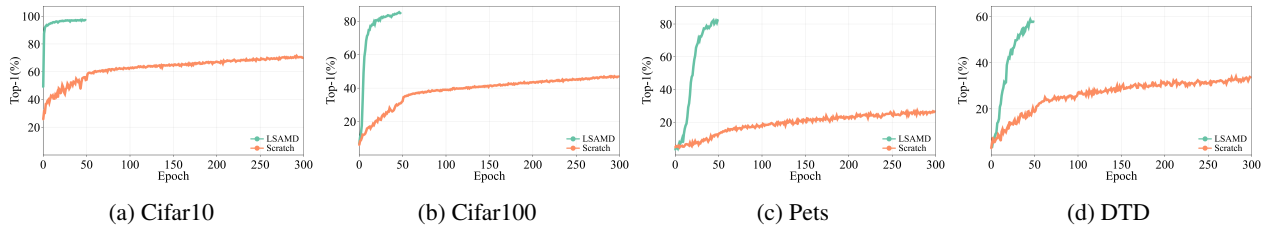


Figure 6: Comparison of Scratch and LSAMD on 10-layer Des-Nets across 4 downstream dataset.

Layer	Params(M)	FLOPs(G)	LG-Params(M)	LSAMD					
				Cifar100	Cifar10	Tiny-IMNet	INAT-2019	Food-101	DTD
5	36.11	7.09	36.11	80.93	95.70	71.53	50.26	58.68	52.39
6	43.20	8.49		81.24	95.94	70.97	53.49	57.08	53.62
7	50.28	9.89		82.25	96.59	72.39	54.26	59.17	54.20
8	57.37	11.28		83.78	96.74	73.27	56.57	63.81	58.56
9	64.46	12.68		84.63	97.30	74.63	58.92	65.96	59.47
10	71.55	14.07		85.40	97.46	76.40	61.85	67.35	58.67
11	78.64	15.47		85.52	97.59	75.98	64.72	64.36	55.69
12	85.72	16.86		83.86	97.70	76.62	65.70	64.21	57.61
13	92.81	18.26		77.64	97.70	77.06	64.74	60.71	55.53
14	99.90	19.65		86.18	97.65	77.56	65.52	62.29	56.78
15	106.99	21.05		85.77	97.97	77.41	66.28	65.72	57.07

Table 2: The results of variable-sized Des-Nets on multiple downstream image classification datasets and comparison of storage resource costs between training from scratch and LSAMD. ‘Layer’ means the number of layers in the Des-Nets, and ‘LG-Params’ is number of parameters of the extracted learngene.

trated in Figure 6, the LSAMD-initialized Des-Net significantly outperforms the Scratch across all datasets. Moreover, even after 300 epochs of training, the Scratch shows limited improvement on downstream datasets with smaller sample sizes. In contrast, the LSAMD-initialized Des-Nets achieve superior performance after 50 epochs, highlighting its ability to enhance performance on datasets with fewer samples. These results underscore the advantages of LSAMD over training from scratch on both classification and segmentation tasks.

**LSAMD vs. PF.** We also compare LSAMD against the pretrain-finetune (PF) method, which **serves as an upper bound**. PF trains the Des-Net on ImageNet-1K for 100 epochs and then finetunes the Des-Net on downstream datasets for 50 epochs. **In contrast, LSAMD directly trains the Des-Net for 50 epochs.** Figure 5 presents a performance comparison of the Des-Net trained using PF, Scratch, and LSAMD over 50 epochs, with evaluations recorded every 5 epochs. The performance of LSAMD is significantly lower than that of PF at the beginning. However, as training progresses, the performance of LSAMD gradually approaches that of PF and ultimately achieves comparable results by the end of training. For example, on the Cifar10 dataset, the performance gap between LSAMD and PF decreases from 47.16% at the start of training to 0.87% by the end. Similarly, on the Cifar100 dataset, the gap reduces from 61.2% to 3.66%. These findings demonstrate that LSAMD effectively enhances the training efficiency and

performance of Des-Net.

**LSAMD vs. SWS/TLEG.** To evaluate the effectiveness of extracting learngene using multiple datasets versus a single dataset, we compared LSAMD with a part of earlier Learngene methods: SWS and TLEG for the following reasons. While Van-LG and Auto-LearnGene are designed for CNN or ViT architectures, LSAMD is conducted on the DeiT architecture. Additionally, PEG and LearnGene Pool report results for DeiT-Ti/S on the downstream datasets, whereas LSAMD primarily focuses on DeiT-B. Therefore, SWS and TLEG were chosen for comparison. For consistency, we compared LEG with SWS and TLEG under the same settings. Table 1 shows results on four downstream datasets of 6, 7, 8-layer Des-Nets initialized by LSAMD and SWS/TLEG. LSAMD outperforms all other methods on all datasets. For example, LSAMD exceeds TLEG by 4.23% on the Cifar100 dataset with a 6-layer Des-Net. Although SWS and TLEG use the larger ImageNet-1K dataset to extract learnGene, using multiple smaller datasets outperforms them on most downstream datasets. **This result confirms that extracting learnGene by multiple datasets yields better performance than using a single large dataset.**

**Comparison of storage and training costs between LSAMD and PF.** As mentioned above, the Pretrain-Finetune (PF) method is both time-consuming and storage-demanding. In this section, we provide a detailed comparison of the training time and storage costs between LSAMD and PF. Specifically, LSAMD requires fewer training epochs

	Cifar100	Cifar10	Ti-IMNet	INAT2019	Food101	Cars196	Flowers102	Pets	DTD	Caltech101
Batch	<b>90.71</b>	<b>98.61</b>	<b>91.41</b>	58.21	<b>80.92</b>	<b>86.41</b>	<b>94.20</b>	<b>85.29</b>	<b>75.43</b>	<b>99.65</b>
Img	87.13	95.29	84.28	<b>59.87</b>	61.14	55.45	91.27	83.16	70.48	97.12

Table 3: Performance comparison of two forward propagation methods for input batch data. ‘Batch’ means that entire batch of data selects one block for forward propagation, and ‘Img’ denotes that each sample in one batch independently forwards to the corresponding blocks according to the probability.

Dataset	Des-Net with 6 layers			Des-Net with 7 layers		
	First	Middle	Last	First	Middle	Last
Cifar100	81.24	82.29	<b>82.77</b>	83.09	83.46	<b>84.38</b>
Cifar10	95.94	96.00	<b>96.67</b>	96.65	97.00	<b>97.42</b>
Ti-IMNet	70.97	72.01	<b>73.59</b>	72.66	72.39	<b>74.70</b>
Food101	57.08	59.73	<b>63.27</b>	58.38	61.11	<b>65.64</b>
Pets	67.33	75.23	<b>79.86</b>	72.07	76.43	<b>81.34</b>
DTD	53.62	<b>55.37</b>	54.84	53.72	53.94	<b>56.91</b>
Caltech101	43.55	48.68	<b>50.46</b>	45.05	47.35	<b>53.80</b>

Table 4: Comparison of the Des-Net with 6 and 7 layers expanded by three priority expansion stages. ‘First’/‘Middle’/‘Last’ are first/middle/last-stage priority.

than PF. For example, when applied to five Des-Nets across a single downstream dataset, LSAMD reduces training costs by approximately **1.36×** compared to PF ( $50 \times 10 + 50 \times 5$  epochs vs.  $150 \times 5$  epochs). It is important to note that the model is pretrained for 100 epochs and fine-tuned for 50 epochs per dataset, and the cost savings become more pronounced as the scale of Des-Nets increases. Furthermore, we compare the storage requirements of PF and LSAMD, as shown in Table 2. LSAMD achieves a substantial reduction in storage costs, saving **95.41%** of the storage space required by PF (36.11M vs. 787.03M). This significant saving is attributed to the fact that PF stores all parameters of variable-sized pre-trained models, whereas LSAMD only stores the learnings.

**Performance of variable-sized Des-Nets.** We start from learnings layers and use them to initialize Des-Nets with different scales. Table 2 shows the performance of these variable-sized Des-Nets across six datasets. The results indicate that the performance of each Des-Net is stable and generally improves with an increase in the number of parameters. This demonstrates the effectiveness and flexibility of the proposed LSAMD method for building variable-sized Des-Nets for various resource constraints.

### Ablation Studies

As previously mentioned, there are two methods for propagating input batch data through each layer of the Ans-Net: 1) In the ‘Batch’ method, the entire batch data is forwarded through either the base block or the dataset-related block, based on the probability value calculated by DAD. 2) In the ‘Img’ method, each sample in the batch independently selects a block for propagation, either the base block or the dataset-related block.

We compared the performance of these methods across

multiple datasets, as shown in Table 3. The ‘Batch’ method generally outperforms the ‘Img’ method on almost all datasets. Notably, the ‘Batch’ method shows performance improvements of 19.78% and 30.96% over ‘Img’ on the Food101 and Cars196 datasets, respectively. This improvement may be due to the ‘Img’ method splitting the batch into two subsets, with only one subset used for the dataset-related blocks, resulting in less data for training these blocks compared to the ‘Batch’ method. Consequently, ‘Img’ tends to exhibit lower performance. The effect of the ‘Batch’ and ‘Img’ methods on base block selection is further discussed in the supplementary material.

**Various priority expansion stages.** In the expansion phase, there are three potential priority positions: first, middle, and last. Here, we conducted experiments to evaluate the impact of these positions on the performance of the Des-Nets. For a 6-layer Des-Net with learnings layers indexed at (1, 4, 5, 7, 8), the indexes after applying first-stage, middle-stage, and last-stage priority expansions are (1, **1**, 4, 5, 7, 8), (1, 4, 5, **5**, 7, 8), and (1, 4, 5, 7, 8, **8**), respectively. The results, presented in Table 4, show that Des-Nets with last-stage priority expansion generally outperform those with other priority positions across most datasets, while those with middle-stage priority expansion rank second. Based on the results from adding one layer, we further investigate the priority of adding multiple layers. Specifically, we present the results for 7-layer Des-Nets, where the indexes for priority expansions in middle-first-stage, last-first-stage, and last-middle-stage orders are (1, **1**, 4, 5, **5**, 7, 8), (1, **1**, 4, 5, 7, 8, **8**), and (1, 4, 5, **5**, 7, 8, **8**), respectively. As shown in Table 4, the last-middle-stage priority expansion yields the best results across all 7 datasets, while the last-first-stage expansion ranks second on most datasets. These findings confirm that expanding at the last stage, followed by the middle stage and then the first stage, leads to progressively improved performance.

### Conclusion

This paper introduces LSAMD, a novel method for building variable-sized Des-Nets for different resource constraints. Initially, LSAMD integrates a dataset-specific block and a DAD module into each layer of the Ans-Net to construct the super Ans-Net. The super Ans-Net is then trained on multiple datasets, updating the parameters of the dataset-specific blocks while keeping the base block fixed. During training, the DAD module learns to search between the dataset-related and base blocks based on probabilities. The base blocks most frequently selected across datasets are extracted

as learngene layers. These learngene layers are subsequently expanded to build Des-Nets of different scales, with priorities set in the order of last-middle-first. Experimental results on multiple datasets validate the superior performance of LSAMD.

## References

- Akbari, H.; Kondratyuk, D.; Cui, Y.; Hornung, R.; Wang, H.; and Adam, H. 2023. Alternating Gradient Descent and Mixture-of-Experts for Integrated Multimodal Perception. *ArXiv*, abs/2305.06324.
- Bossard, L.; Guillaumin, M.; and Gool, L. V. 2014. Food-101 - Mining Discriminative Components with Random Forests. In *European Conference on Computer Vision*.
- Chen, G.; Zhao, X.; Chen, T.; and Cheng, Y. 2024.  $\{\text{MoE-RBench}\}$ : Towards Building Reliable Language Models with Sparse Mixture-of-Experts.
- Chen, Z.; Shen, Y.; Ding, M.; Chen, Z.; Zhao, H.; Learned-Miller, E. G.; and Gan, C. 2022. Mod-Squad: Designing Mixture of Experts As Modular Multi-Task Learners. *ArXiv*, abs/2212.08066.
- Cimpoi, M.; Maji, S.; Kokkinos, I.; Mohamed, S.; and Vedaldi, A. 2013. Describing Textures in the Wild. *2014 IEEE Conference on Computer Vision and Pattern Recognition*, 3606–3613.
- Deng, J.; Dong, W.; Socher, R.; Li, L.-J.; Li, K.; and Fei-Fei, L. 2009. ImageNet: A large-scale hierarchical image database. *2009 IEEE Conference on Computer Vision and Pattern Recognition*, 248–255.
- Dosovitskiy, A.; Beyer, L.; Kolesnikov, A.; Weissenborn, D.; Zhai, X.; Unterthiner, T.; Dehghani, M.; Minderer, M.; Heigold, G.; Gelly, S.; Uszkoreit, J.; and Houlsby, N. 2020. An Image is Worth 16x16 Words: Transformers for Image Recognition at Scale. *ArXiv*, abs/2010.11929.
- Everingham, M.; Eslami, S. A.; Van Gool, L.; Williams, C. K.; Winn, J.; and Zisserman, A. 2015. The pascal visual object classes challenge: A retrospective. *International journal of computer vision*, 111(1): 98–136.
- Fedus, W.; Zoph, B.; and Shazeer, N. 2022. Switch transformers: Scaling to trillion parameter models with simple and efficient sparsity. *Journal of Machine Learning Research*, 23(120): 1–39.
- Fei-Fei, L.; Fergus, R.; and Perona, P. 2004. Learning Generative Visual Models from Few Training Examples: An Incremental Bayesian Approach Tested on 101 Object Categories. *2004 Conference on Computer Vision and Pattern Recognition Workshop*, 178–178.
- Horn, G. V.; Aodha, O. M.; Song, Y.; Cui, Y.; Sun, C.; Shepard, A.; Adam, H.; Perona, P.; and Belongie, S. J. 2017. The iNaturalist Species Classification and Detection Dataset. *2018 IEEE/CVF Conference on Computer Vision and Pattern Recognition*, 8769–8778.
- Jacobs, R. A.; Jordan, M. I.; Nowlan, S. J.; and Hinton, G. E. 1991. Adaptive Mixtures of Local Experts. *Neural Computation*, 3: 79–87.
- Krause, J.; Stark, M.; Deng, J.; and Fei-Fei, L. 2013. 3D Object Representations for Fine-Grained Categorization. *2013 IEEE International Conference on Computer Vision Workshops*, 554–561.
- Krizhevsky, A. 2009. Learning Multiple Layers of Features from Tiny Images.
- Le, Y.; and Yang, X. S. 2015. Tiny ImageNet Visual Recognition Challenge.
- Lin, B.; Tang, Z.; Ye, Y.; Cui, J.; Zhu, B.; Jin, P.; Zhang, J.; Ning, M.; and Yuan, L. 2024. MoE-LLaVA: Mixture of Experts for Large Vision-Language Models. *ArXiv*, abs/2401.15947.
- Liu, Z.; Chen, K.; Han, J.; Hong, L.; Xu, H.; Li, Z.; and Kwok, J. T.-Y. 2024. Task-customized Masked Autoencoder via Mixture of Cluster-conditional Experts. *ArXiv*, abs/2402.05382.
- Nilsback, M.-E.; and Zisserman, A. 2008. Automated Flower Classification over a Large Number of Classes. *2008 Sixth Indian Conference on Computer Vision, Graphics & Image Processing*, 722–729.
- Parkhi, O. M.; Vedaldi, A.; Zisserman, A.; and Jawahar, C. V. 2012. Cats and dogs. *2012 IEEE Conference on Computer Vision and Pattern Recognition*, 3498–3505.
- Riquelme, C.; Puigcerver, J.; Mustafa, B.; Neumann, M.; Jenatton, R.; Pinto, A. S.; Keyzers, D.; and Houlsby, N. 2021. Scaling Vision with Sparse Mixture of Experts. In *Neural Information Processing Systems*.
- Shazeer, N. M.; Mirhoseini, A.; Maziarz, K.; Davis, A.; Le, Q. V.; Hinton, G. E.; and Dean, J. 2017. Outrageously Large Neural Networks: The Sparsely-Gated Mixture-of-Experts Layer. *ArXiv*, abs/1701.06538.
- Shi, B.; Xia, S.; Yang, X.; Chen, H.; Kou, Z.; and Geng, X. 2024. Building Variable-Sized Models via LearnGene Pool. In *Proceedings of the AAAI Conference on Artificial Intelligence*, volume 38, 14946–14954.
- Touvron, H.; Cord, M.; Douze, M.; Massa, F.; Sablayrolles, A.; and Jégou, H. 2020. Training data-efficient image transformers & distillation through attention. In *International Conference on Machine Learning*.
- Wang, Q.; Yang, X.; Chen, H.; and Geng, X. 2024. Vision Transformers as Probabilistic Expansion from LearnGene. In *Forty-first International Conference on Machine Learning*.
- Wang, Q.; Yang, X.; Lin, S.; and Geng, X. 2023. LearnGene: Inheriting Condensed Knowledge from the Ancestry Model to Descendant Models. *ArXiv*, abs/2305.02279.
- Wang, Q.-F.; Geng, X.; Lin, S.-X.; Xia, S.-Y.; Qi, L.; and Xu, N. 2022. LearnGene: From open-world to your learning task. In *Proceedings of the AAAI Conference on Artificial Intelligence*, volume 36, 8557–8565.
- Wu, L.; Liu, M.; Chen, Y.; Chen, D.; Dai, X.; and Yuan, L. 2022. Residual Mixture of Experts. *ArXiv*, abs/2204.09636.
- Xia, S.; Zhang, M.; Yang, X.; Chen, R.; Chen, H.; and Geng, X. 2024a. Transformer as Linear Expansion of LearnGene. In *Proceedings of the AAAI Conference on Artificial Intelligence*, volume 38, 16014–16022.

Xia, S.; Zu, Y.; Yang, X.; and Geng, X. 2024b. Initializing variable-sized vision transformers from learngene with learnable transformation. *Advances in Neural Information Processing Systems*, 37: 43341–43366.

Xia, S.-Y.; Zhu, W.; Yang, X.; and Geng, X. 2024c. Exploring LearnGene via Stage-wise Weight Sharing for Initializing Variable-sized Models. *arXiv preprint arXiv:2404.16897*.

Ye, H.; and Xu, D. 2023. TaskExpert: Dynamically Assembling Multi-Task Representations with Memorial Mixture-of-Experts. *2023 IEEE/CVF International Conference on Computer Vision (ICCV)*, 21771–21780.

Zhou, B.; Zhao, H.; Puig, X.; Fidler, S.; Barriuso, A.; and Torralba, A. 2017. Scene Parsing through ADE20K Dataset. In *Proceedings of the IEEE Conference on Computer Vision and Pattern Recognition*.

Zhou, B.; Zhao, H.; Puig, X.; Xiao, T.; Fidler, S.; Barriuso, A.; and Torralba, A. 2019. Semantic understanding of scenes through the ade20k dataset. *International Journal of Computer Vision*, 127(3): 302–321.

## Appendix

We organize the appendix as follows.

- In Section , we provide the detailed hyper-parameters and hardware during training.
- In Section , we list the information of the ten selected datasets for learnGene extraction.
- In Section , we show the impact of the ‘Batch’ and ‘Img’ methods on the base block selection in the supplementary material.

### Hyper-parameters and Hardware

We adopt a total batch size of 128 on 4 3090 GPUs. The initial learning rates for learnGene extraction on each task and fine-tuning the built descendant models on the downstream datasets are shown in Table 5. In the above two training processes, the learning rate decay strategy is the poly method.

### Datasets for LearnGene Extraction

We show the overview information of ten datasets for training the redesigned Ans-Net to extract learnGene layers in Table 6.

### The Impact of the ‘Batch’ and ‘Img’ Methods on the Base Block Selection

To verify the impact of the ‘Batch’ method on the base block selection, we also show the indices of base blocks selected in the ‘Batch’ and ‘Img’ propagation methods on all datasets in Figure 7. We can find that the base blocks selected by the both methods on each task are highly overlapped. Although the ‘Img’ method has been proven to be valid by Mod-Squad, ‘Batch’ has better performance in training Ans-Net While achieving almost the same selection results as ‘Img’. This further verifies the superiority of the ‘Batch’ in selecting base blocks.

Datasets	Ans-Net	Des-Net
Cifar100	5.00E-04	5.00E-04
Cifar10	1.00E-06	5.00E-04
Tiny-ImageNet	1.00E-05	5.00E-04
INAT2019	1.00E-05	5.00E-05
Food101	1.00E-05	1.00E-05
Cars196	5.00E-04	1.00E-05
Flowers102	5.00E-04	1.00E-04
Pets	1.00E-05	1.00E-04
DTD	1.00E-04	1.00E-05
Caltech101	1.00E-05	1.00E-05
ADE-20K	1.00E-05	1.00E-05
VOC12	1.00E-05	1.00E-05

Table 5: The initial learning rates for training the Ans-Net and fine-tuning the Des-Nets on ten datasets. ‘E-04’ represents  $10^{-4}$ .

Dataset	Categories	Training	Testing
CIFAR-100	100	50000	10000
CIFAR-10	10	50000	10000
Tiny-ImageNet	200	100000	10000
INAT2019	1010	268243	64401
Food101	101	75750	25250
Car196	196	8144	8041
Flowers102	102	2040	818
Pets	37	3680	3669
DTD	47	3760	1880
Caltech101	101	6942	1735
ADE-20K	150	20210	200
VOC12	20	10582	1449

Table 6: The overview information of ten datasets for training the redesigned Ans-Net to extract learnGene layers

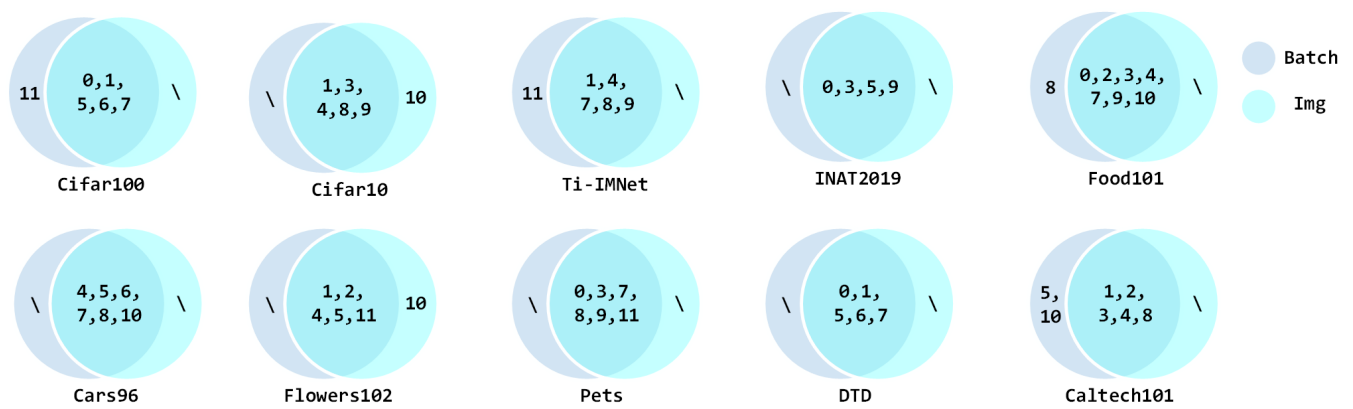


Figure 7: The intersection of the indexes of the base blocks selected by the ‘Batch’ and ‘Img’ propagation methods. ‘\’ means the null value.